

# Lithium-Sulfur-Batteries under Lean Electrolyte Conditions: Improving Rate Capability by the Choice of the Lithium Salt in Dimethoxyethane-Hydrofluoroether-Based Electrolyte

Sebastian Kirchhoff,<sup>[a, b]</sup> Paul Härtel,<sup>[b]</sup> Susanne Dörfler,\*<sup>[b]</sup> Thomas Abendroth,<sup>[b]</sup> Holger Althues,<sup>[b]</sup> and Stefan Kaskel<sup>[a, b]</sup>

Lithium-sulfur batteries (LSBs) are discussed as the most promising post-lithium-ion battery technology due to the high theoretical energy density and the cost-efficient, environmental-friendly active material sulfur. Unfortunately, LSBs still suffer from several limitations such as cycle life and rate capability. To overcome these issues, the development of adapted electrolytes is one promising path. Consequently, in this study, we focus on the influence of the lithium salt on the performance of LSBs. In a fixed solvent system without employing LiNO<sub>3</sub>, five different lithium salts are compared. The electrolyte properties as well as the influence of polysulfides are determined and discussed in relation with the battery performance. Interest-

ingly, although the different salts lead to different electrolyte properties, only a minor influence of the salt is observed at low C-rates. By performing a rate capability test, however, a strong influence of the lithium salt is detected at high C-rates, with LiFSI outperforming the other salts. This correlates well with ionic conductivity and a suppressed influence of polysulfides in case of LiFSI. To verify the results, multi-layered pouch cells were tested under lean electrolyte conditions. The study emphasizes the significance of the lithium salt and provides guidance for electrolyte design under lean electrolyte conditions.

## Introduction

The transformation to a CO<sub>2</sub>-neutral world requires the application of energy storage devices. Lithium-sulfur-batteries (LSBs) are currently discussed as a promising and sustainable solution since sulfur is cost-efficient, abundant and non-toxic, which is a strong advance in comparison to state of the art (SOTA) Li-ion battery cathode materials.<sup>[1]</sup> In addition, both electrode materials, sulfur (1672 mAh/g) and lithium (3860 mAh/g) show exceptionally high theoretical specific capacities.<sup>[1,2]</sup> Therefore, recent advances especially in terms of cathode development have already enabled prototype cells with specific energies from over 400 Wh/kg,<sup>[3]</sup> making LSBs attractive especially for flight applications, like drones or high altitude pseudo satellites (HAPS).<sup>[4]</sup> Unfortunately, so far LSBs still suffer from several limitations, namely

cycle life as well as rate capability, which hinders their commercialization.<sup>[5]</sup> Limitations in terms of cycle life arises mainly through degradation reactions at the lithium metal anode, where electrolyte decomposition as well as the so-called polysulfide (PS) shuttle phenomena take place.<sup>[6,7]</sup> In order to prevent the challenge of polysulfide shuttle, several solutions were proposed in literature, including e.g. anchoring sulfur in the cathode structure (in micropores<sup>[8]</sup> or in SPAN-structure<sup>[9,10]</sup>), the use of protection layers on the anode<sup>[11]</sup> or the separator.<sup>[12]</sup> However, these solutions have also several disadvantages such as low S-loading, decreased cell voltage or additional cost and weight in case of additional protection layers. Thus, in order to address both issues, the development of adapted electrolytes for lithium sulfur batteries has been discussed as more promising. In addition to the mentioned challenges, the electrolyte also influences the rate capability of the cell especially under lean electrolyte conditions.<sup>[13]</sup> The SOTA-electrolyte DME/DOL (1/1) (1,2-dimethoxyethane/1,3-dioxolane) containing 1 M LiTFSI (lithium bis(trifluoromethanesulfonyl)imide) and LiNO<sub>3</sub> as additive (DME/DOL) has been so far still the electrolyte of choice in most publications since the performance especially in coin cells with high electrolyte excess is quite decent.<sup>[7]</sup> This can be related to the high solvating ability of the solvents, which results in a high ionic conductivity of the electrolyte as well as high polysulfide solubility, which can increase the kinetics.<sup>[14]</sup> Unfortunately, when applying lean electrolyte conditions in order to achieve high energy densities, such electrolytes with high PS-solubility show limited performance as the viscosity of the dissolved polysulfides mainly determines the rate capability.<sup>[13]</sup> In addition,

[a] S. Kirchhoff, Prof. Dr. S. Kaskel

Chair of Inorganic Chemistry I

TU Dresden

Bergstrasse 66, 01069 Dresden, Germany

[b] S. Kirchhoff, P. Härtel, Dr. S. Dörfler, Dr. T. Abendroth, Dr. H. Althues,

Prof. Dr. S. Kaskel

Technology field Chemical Surface Technology

Fraunhofer Institute for Material and Beam technology (IWS)

Winterbergstrasse 28, 01277 Dresden, Germany

E-mail: susanne.doerfler@iws.fraunhofer.de

 Supporting information for this article is available on the WWW under <https://doi.org/10.1002/batt.202400155>

 © 2024 The Authors. Batteries & Supercaps published by Wiley-VCH GmbH. This is an open access article under the terms of the Creative Commons Attribution License, which permits use, distribution and reproduction in any medium, provided the original work is properly cited.

to prevent the PS-shuttle, the use of  $\text{LiNO}_3$  as electrolyte additive is necessary.<sup>[15]</sup> However,  $\text{LiNO}_3$  is continuously consumed during cycling and leads additionally to strong gas formation, thus creating a huge safety risk.<sup>[16,17]</sup> To overcome these obstacles accompanying high PS-solubility, another class of electrolytes, so-called sparingly polysulfide solvating electrolytes (SPSEs),<sup>[18]</sup> have been developed. By using long chain-ethers,<sup>[19,20]</sup> fluoroethers<sup>[21,22]</sup> and/or high salt concentrations,<sup>[23]</sup> the PS-solubility in the electrolyte is successfully minimized, leading to a reduced shuttle phenomena and enabling cycle stability at low electrolyte amounts. Previously, our group published stable cycling of a pouch cell comprising TMS/TTE with 1.5 M LiTFSI as electrolyte with an E:S ratio as low as 2.57  $\mu\text{l}/\text{mg-S}$ .<sup>[16]</sup> Lean electrolyte conditions are mandatory in order to achieve high gravimetric energy densities of LSBs since so far in most cases the electrolyte shows the highest weight proportion of the cell with at least 35 %.<sup>[24]</sup> Unfortunately, the condition of a low polysulfide dissolution correlates very often with limited conversion kinetics, which is then challenging for possible practical applications.<sup>[7]</sup> Thus, a compromise between SPSEs and highly solvating electrolytes must be found to pave the path for the LSB commercialization. Recently, various new electrolyte compounds, including solvents, salts and additives have been proposed in literature.<sup>[10,25]</sup> However, as every research group uses its own cathode composition and areal loading and different testing parameters<sup>[24]</sup> the results are often difficult to classify or rather to compare. In addition, some publications also did not add a reference electrolyte, which further hampers fair comparison. Regarding the lithium salts, different types of salts have been introduced in the literature.<sup>[26]</sup> In general, conventional salts like  $\text{LiCl}$ ,  $\text{LiF}$  or  $\text{Li}_2\text{O}$  are not purposeful due to the low solubility in aprotic solvents and therefore also low kinetics in the cell.<sup>[26]</sup> Phosphate- and fluorophosphorous acid ester-based lithium salts and additives usually applied in LIB-electrolytes are not suitable for LSBs due to the nucleophilic decomposition by polysulfides.<sup>[27]</sup> Thus, especially imide-based salts are applied in LSBs due to their relatively high stability against lithium and polysulfides as well as their quite high dissociation in aprotic solvents.<sup>[14]</sup> Some studies on the influence of the lithium salt have been already carried out. However, usually DME/DOL is used as solvent system, which in turn needs  $\text{LiNO}_3$  as additive.<sup>[28]</sup> Consequently, the effect of the actual lithium salt is reduced or not clear. Otherwise, without using  $\text{LiNO}_3$ , strong PS-shuttle occurs, which would again limit the validity of the cycling performance.<sup>[29]</sup> Thus, to the best of our knowledge, a comparative study showing the real influence of the lithium salt with rational solvent adaption on the rate capability, discharge capacity and cycle stability has not been carried out yet.

Herein, we present a study regarding the influence of the lithium salt on electrolyte properties as well as cycling performance in LSBs. We have chosen five different salts for our study, which are already known in literature to show decent stability in LSBs: LiTFSI, LiFSI (lithium bis(fluorosulfonyl)imide), LiBETI (lithium

bis(pentafluoroethanesulfonyl)imide), LiTf (lithium trifluoromethanesulfonate) and LiTDI (lithium 2-trifluoromethyl-4,5-dicyanoimidazolide) in a solvent blend of DME/TTE in a ratio of 1/1. This enables cycling by circumventing the use of  $\text{LiNO}_3$ .

This study shows that – although the intrinsic uncycled electrolyte properties differ markedly – the cycling performance at 0.1 C is quite similar, whereas the rate capability is strongly influenced by the choice of lithium salt and related to the ionic conductivity of the electrolytes. In addition, by studying the influence of polysulfide saturation on the electrolyte properties, we identify LiFSI showing a unique behavior since viscosity as well as ionic conductivity is not affected by polysulfides. To verify the rate capability results under lean conditions, multi-layered pouch cells were built and evaluated under lean electrolyte conditions (E:S = 3  $\mu\text{l}/\text{mg-S}$ ), which underline the beneficial properties of LiFSI in comparison to reference LiTFSI also under practical conditions.

## Results and Discussion

### Electrolyte Characterization

In order to screen different lithium salts for their influence on the sulfur cathode chemistry, a sensible solvent mixture needed to be found as DME/DOL as SOTA-solvent ratio leads to a stark polysulfide shuttle effect. The addition of  $\text{LiNO}_3$  to a DME/DOL mixture would additionally mask the results. Hence, the fluoroether TTE was chosen in order to balance the polysulfide shuttle and the need of polysulfides for an enhanced kinetics. DOL, however, did not solve all potential salts LiTFSI, LiFSI, LiBETI, LiTf and LiTDI (shown in Figure 1) to the same degree or leads to electrolyte decomposition in case of LiFSI.<sup>[30]</sup> Finally, DME was selected as it dissolves all lithium salts to the same degree (1 M) and matches well with TTE and the sulfur cathode chemistry. The DME/TTE ratio 1/1 is a compromise between a high salt solubility and high ionic conductivity delivered by DME and a reduced PS-solubility and accompanied reduced PS-shuttle due to the fluoroether TTE. Likewise, the addition of an additive such as  $\text{LiNO}_3$ , which is consumed over cycling, is not necessary. In recent studies, the combination of DME, LiFSI and a fluoroether already lead to promising results especially in terms of lithium anode stability but also high coulombic efficiencies in LSBs could be achieved by the adaption of electrolyte composition.<sup>[31,32]</sup> Thus, the electrolyte composition is highly suitable for a study of the influence of the lithium salt. Further possible solvents which might show high solvating abilities for all salts like glymes or sulfolane show higher viscosities and therefore reduced ionic conductivity<sup>[33,34]</sup> or in case of DMF or DMSO strong instability against lithium and were therefore excluded.<sup>[35]</sup>

In order to understand the influence of the lithium salt, firstly the properties of the pristine, uncycled electrolytes were determined at 25 °C, as shown in Table 1 and Figure 2. The electrolyte (mass) density (Table 1) is an often-neglected property. However, since the electrolyte has in general the

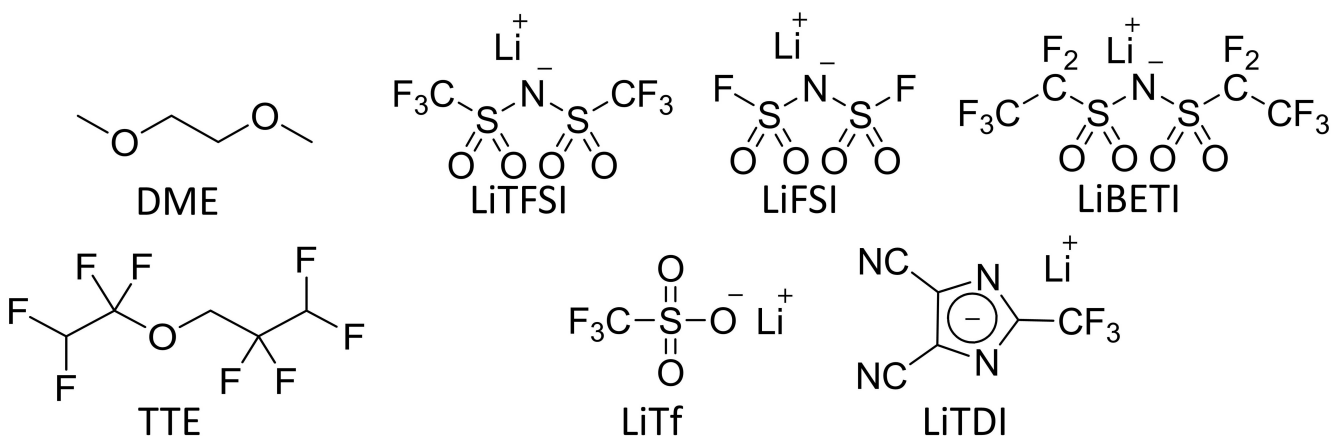


**Figure 1.** Molecular structures of the electrolyte compounds: DME (1,2-dimethoxyethane), TTE (1,1,2,2-tetrafluoroethyl 2,2,3,3-tetrafluoropropyl ether), LiTFSI (lithium bis(pentafluoroethanesulfonyl)imide) LiFSI (lithium bis(fluorosulfonyl)imide), LiBETI (lithium bis(pentafluoroethanesulfonyl)imide), LiTf (lithium trifluoromethanesulfonate), LiTDI (lithium 2-trifluoromethyl-4,5-dicyanoimidazolidine).

<b>Table 1.</b> Electrolyte densities at 25 °C, in DME:TTE 1/1, 1 M lithium salt.	
Lithium salt	$\rho$ [g/cm <sup>3</sup> ]
LiTFSI	1.31
LiFSI	1.29
LiBETI	1.35
LiTf	1.26
LiTDI	1.21

highest weight proportion of the cell, the electrolyte density will drastically influence the gravimetric energy density. The densities of the five different electrolyte solutions are quite similar with values between 1.22 g/cm<sup>3</sup> (LiTDI) and 1.35 g/cm<sup>3</sup> (LiBETI).

Consequently, the influence of the solvent system is here more important than the lithium salt used. This behavior might change in case of higher salt concentrations. The determined densities in the range of 1.3 g/cm<sup>3</sup> are in the medium regime compared to other LSB-electrolytes. In comparison SOTA-DME/DOL-electrolyte has a density of 1.2 g/cm<sup>3</sup>,<sup>[24]</sup> whereas several other electrolytes such as TMS:TTE or high concentrated electrolytes show higher densities of 1.5 g/cm<sup>3</sup> and above.<sup>[19,36]</sup>

Since the salt concentration applied here is in medium range (1–1.5 M) and DME has a very low density of 0.87 g/cm<sup>3</sup>, the higher density is mainly caused by the high density of the fluoroether, TTE ( $\rho = 1.5$  g/cm<sup>3</sup>).<sup>[37]</sup> The electrolyte density solely influences the external properties of the battery, whereas the following determined properties directly influence the cell kinetics, and the importance of the electrolyte viscosity and ionic conductivity is even higher. In case of LSBs, a further electrolyte property plays also a decisive role, the polysulfide solubility. As polysulfides are formed during cycling and dissolve in the electrolyte they also influence the properties of the electrolyte.<sup>[13,17,38]</sup> This might be no issue in case of coin cells, however, testing in pouch cells and under lean electrolyte conditions the change of properties can strongly influence the cell performance depending on the electrolyte.<sup>[13]</sup> Thus, in addition to the properties of the pure electrolyte, the properties of polysulfide-saturated solutions were determined: electrolyte solutions saturated with polysulfides were prepared by adding Li<sub>2</sub>S and S<sub>8</sub> in excess to the electrolyte and filtering off the precipitation. Subsequently, the polysulfide solubility was determined gravimetrically and the obtained solutions were also characterized in terms of electrolyte viscosity and ionic

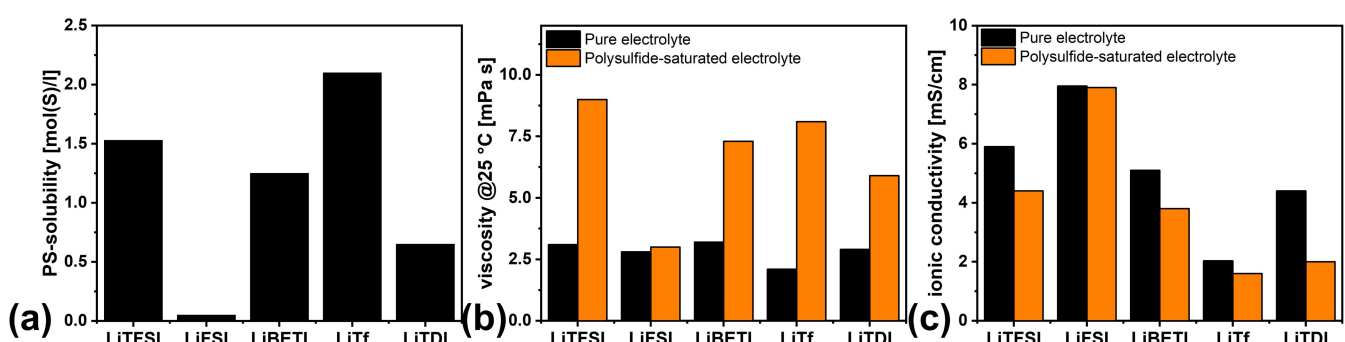


**Figure 2.** Physicochemical characterization at 25 °C of the electrolytes with varying lithium salt, DME/TTE 1/1 with 1 M lithium salt: (a) PS-solubility of the electrolytes, determined gravimetrically, (b) viscosity of pristine and PS-saturated electrolytes, (c) ionic conductivity of pristine and PS-saturated electrolytes.

conductivity, and the resulting data are plotted in the same graph (Figure 2(a)–2(c)).

Previous studies by other groups have already shown that lithium salts influence the polysulfide solubility of the electrolyte. According to the literature, LiTf shows a higher polysulfide solubility than LiTFSI<sup>[39]</sup> whereas LiTDI can reduce polysulfide solubility in comparison to LiTFSI.<sup>[40]</sup> In case of LiTf, the higher PS-solubility can be related to the higher donor number of the Tf-anion in comparison to TFSI<sup>-</sup>.<sup>[41]</sup> For LiTDI, no donor number was reported and the restricted PS-solubility might be related to the formation of larger agglomerates of PS.<sup>[40]</sup> To validate these findings also for the electrolyte system in this study, we determined the total amount of soluble polysulfides via an established gravimetric method by oxidizing polysulfides with H<sub>2</sub>O<sub>2</sub> to sulfate (SO<sub>4</sub><sup>2-</sup>) and precipitating them afterwards with Ba(NO<sub>3</sub>)<sub>2</sub> as BaSO<sub>4</sub> as proposed by Dibden *et al.*<sup>[42]</sup>

The results shown in Figure 2(a) confirm the findings of earlier studies since LiTf leads to a higher polysulfide solubility and LiTDI to a lower PS-solubility than LiTFSI. The polysulfide solubility for LiBETI is slightly lower as for LiTFSI, which is in good agreement to the anionic structure. In comparison to the literature, the electrolytes show higher PS-solubility than before reported SPSEs, like HME/DOL or TMS/TTE.<sup>[38,43]</sup> However, in contrast to highly solvating electrolytes such as LiTFSI in DME/DOL, the PS-solubility is strongly reduced, this is mainly related to the use of TTE as second solvent which is known for marginally coordinating ions. For the LiFSI-electrolyte, the determination of the polysulfide solubility via the gravimetric method was not straightforward as we observed in an initial pre-test with the pure electrolyte also a decomposition of the lithium salt, very likely due to the H<sub>2</sub>O<sub>2</sub> treatment. Given that the anion also contains sulfur in its structure, the determined value would be falsified. Therefore, we determined first the amount of sulfur, that was precipitated from the pure electrolyte (formed through decomposition of the salt anion), and subtracted this value from the following determination of the saturated solution. Interestingly, the determined value was below 0.1 M, which would explain the minor influence of polysulfides on the properties of this electrolyte. However, the reason for this behavior remains unclear. Kim *et al.* observed a similar phenomenon qualitatively by comparing coloration of the PS-solution of a highly concentrated solution (5 M) of LiFSI and LiTFSI in DME/DOL (1/1). This was related to the higher binding energy of TFSI-anions to PS in comparison to FSI.<sup>[30]</sup> Therefore, LiFSI seems to suppress the dissolution of polysulfides in the electrolyte. Corresponding to the different PS-solubilities of the electrolytes also a varying influence of polysulfides on the electrolyte properties could be observed. For the electrolyte viscosity (Figure 2(b), black bars) of the pure electrolyte solutions (without polysulfides), a low influence of the lithium salt, as observed for the electrolyte density, occurs. The viscosities of the pure electrolytes are all around 3 mPas, except the LiTf-based electrolyte, which shows a lower value (2.1 mPas). This is a comparably low value, especially electrolytes with higher salt concentrations or electrolytes comprising solvents with high melting point,

like sulfolane, show higher viscosities.<sup>[44]</sup> In case of polysulfide addition, a strongly enhanced viscosity for four electrolytes is observed. For LiTFSI, LiTDI, LiBETI and LiTf this increase is up to 300%. The LiFSI-electrolyte shows nearly no influence of polysulfides on the viscosity, which is in good agreement with the low PS-solubility. In a previous study, the viscosity data is very strongly influenced by the soluble polysulfides.<sup>[13,38]</sup> As all electrolyte solutions investigated here contain TTE which is known as a viscosity mediator, the polysulfide solubility has only a marginal influence on the viscosity values, in comparison to reported changes of over 5000% in case of conventional DME/DOL-electrolyte.<sup>[13]</sup> However, LiFSI shows also an additional effect with nearly no influence of polysulfides on the viscosity.

Regarding the ionic conductivity, shown in Figure 2(c), clear differences between the salts can be observed. The electrolyte comprising LiTf has the lowest ionic conductivity of 2 mS/cm, which is consistent with literature, due to the lower mesomeric effect regarding anion stabilization and the resulting low dissociation degree of the salt.<sup>[33]</sup> LiTDI shows an ionic conductivity of 4 mS/cm, which is still lower than the values obtained for LiBETI (5.1 mS/cm) and LiTFSI (5.9 mS/cm). By far the highest value shows LiFSI with 8 mS/cm, which can presumably be related to a higher degree of dissociation in combination with a smaller size of the anion.<sup>[45]</sup> In addition, a low influence of PS can be observed also for the ionic conductivity of the LiFSI-electrolyte, which is in good agreement with the observations made for the electrolyte viscosity, resulting in a very promising value of 7.9 mS/cm. Thus, also a decomposition reaction of LiFSI, which could explain the low PS-solubility, in presence of polysulfides can be excluded since the ionic conductivity of the PS-saturated solution, is still similar to the value of the pure electrolyte. In case of decomposition, a drastically decreased value would be expected. Regarding the conductivity, also, LiTf shows only a smaller change of properties, but this might be explained with the already quite low ionic conductivity of the pristine solution. The other electrolytes show a decrease of approx. 25 to 30% in case of LiTFSI and LiBETI and a decrease of 50% for LiTDI.

In conclusion, based on the high ionic conductivity, low viscosity of the pristine electrolyte as well as the low influence of polysulfides on these properties, the LiFSI-electrolyte seems to be the most promising for high rate capability applications. For practically relevant pouch cells with low electrolyte amount, LiTf might be the least promising lithium salt of the five tested here due to its low ionic conductivity in combination with the higher polysulfide solubility, which could result in an increased PS-shuttle.

## Electrochemical Evaluation

In the next step, to further evaluate the influence of the lithium salt, symmetric lithium versus lithium tests were conducted to validate the compatibility of the lithium salts with the lithium metal anode. The tests, performed in coin cells, are shown in Figure 3. Lithium was cycled using a

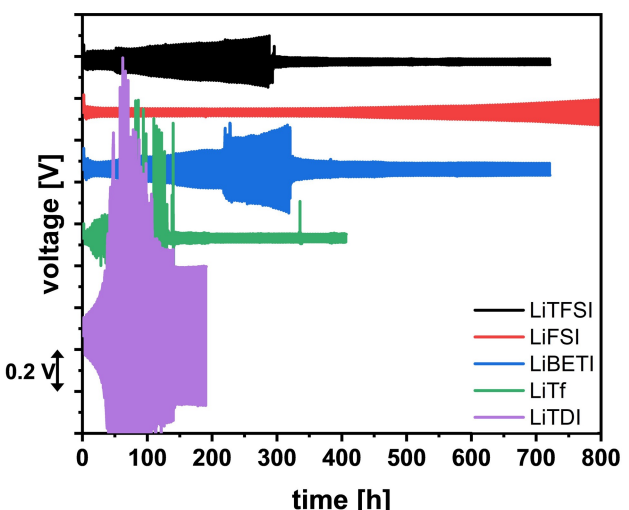


Figure 3. Symmetrical Li/Li tests of the different salt containing electrolytes (DME:TTE 1:1, 1 M lithium salt) using a current density of  $0.5 \text{ mA}/\text{cm}^2$  to reach  $1 \text{ mAh}/\text{cm}^2$  in coin cells at  $25^\circ\text{C}$ .

current of  $0.5 \text{ mA}/\text{cm}^2$  in order to reach a total capacity of  $1 \text{ mAh}/\text{cm}^2$ . The tests were carried out for a maximum of 800 h (in case of LiFSI), which would correspond to 200 cycles. In case of high overpotentials the cells were stopped earlier. Regarding the results, significant differences between the different lithium salts are visible. LiFSI shows by far the best performance reaching the end of cycling after 800 h (200 cycles) with only a slight overpotential. The voltage hysteresis of the last cycle is still only 0.12 V. In contrast to this, the further electrolyte salts did not reach 200 cycles due to earlier cell failure. This is in good agreement with literature, since different LiFSI-electrolytes were proposed recently for stable cycling of lithium metal anodes due to the improved SEI (solid electrolyte interface) formation.<sup>[32,46]</sup> LiTf and LiTDI show the worst performance with strong overpotentials from the beginning and an early cell failure after less than 200 h. This indicates faster electrolyte degradation by the lithium metal anode. In addition, the low ionic conductivity of LiTf might also be a limiting property. LiTFSI and LiBETI show also earlier cell failure than LiFSI after approximately 300 h. However, only a small overpotential is observed in comparison to LiTf and LiTDI, indicating a higher stability of the lithium salt against the lithium metal anode. Overall, the LiFSI-electrolyte seems to be the most stable electrolyte for lithium metal anodes.

However, it is known from our previous study that polysulfides have a drastic influence on the lithium anode performance<sup>[43]</sup> and consequently, the Li vs. Li cycling experiments should not be overestimated. Hence, two types of coin cell testing with a reference sulfur cathode were performed. First tests were conducted by cycling the cells at a constant C-rate of 0.1 C. In a second test, the rate capability of the cells was evaluated in the range of 0.1 C up to 1 C. For the cycling at 0.1 C, we used C/S-cathodes with a sulfur loading of  $2.2 \text{ mg}/\text{cm}^2$ . The results are shown in Figure 4(a) and Figure 4(b),

additional voltage curves can be found in the SI in Figure S1. Interestingly, although the electrolytes differ significantly regarding their ionic conductivity as well as their stability against lithium, the coin cell results are quite similar in terms of capacity retention for the first test at 0.1 C. For all five electrolytes a high sulfur utilization in the first cycle could be obtained with values above  $1000 \text{ mAh/g}$ . The imide-based salts, LiTFSI, LiFSI and LiBETI, lead to nearly the same sulfur utilization of  $1300 \text{ mAh/g}$ . The electrolyte comprising LiTDI leads to a slightly lower value of  $1210 \text{ mAh/g}$  and the use of LiTf results in the lowest utilization of  $1140 \text{ mAh/g}$ . A comparison of the voltage curves of the 5<sup>th</sup> cycle show the similar typical two-plateau profile of LSBs separated by a voltage dip. The voltage dip is more pronounced for LiTDI and especially for LiTf in this cycle. However, with increasing cycle number, the difference between the lithium salts is reduced, indicating only an initial effect. In general, no overpotential is observed for both plateaus no matter which lithium salt used. The capacity loss of all five electrolytes is related to a shortening of the second plateau. This leads over 50 cycles to a capacity retention (referred to cycle 2) of approx. 70% for LiTFSI, LiFSI and LiBETI. LiTDI shows the strongest capacity loss resulting in a capacity retention of 60%. Interestingly, LiTf leads to the highest capacity retention of 75%, which contradicts with the Li vs Li tests, but may be explained with the better Li<sub>2</sub>S-precipitation, enabled by high donor number anions like LiTf,<sup>[47]</sup> and it can be also contributed to the polysulfide species that are known to passivate the lithium anode.<sup>[17,43,48]</sup> However, especially in comparison to the before performed Li vs Li tests, the electrolyte salt seems to have only a minor influence under these conditions on the long-term stability of LSBs. This might be explained by the rather low current of 0.1 C which should be no issue for the electrolytes since even the LiTf-electrolyte with the lowest ionic conductivity of  $2 \text{ mS}/\text{cm}$  has still a higher ionic conductivity than recently reported sparingly solvating electrolytes, like HME/DOL ( $0.9 \text{ mS}/\text{cm}$ )<sup>[19]</sup> or acetonitrile/TTE. ( $1.57 \text{ mS}/\text{cm}$ ).<sup>[21]</sup> Under these conditions, other properties have more impact, e.g. a low viscosity for high cathode wettability, which is fulfilled by all five electrolytes. One difference between the salts can be found in the coulombic efficiency. Whereas LiTFSI, LiBETI show comparatively higher values of 90%, LiTf, LiTDI and LiFSI electrolytes lead to lower values. For the LiTf-electrolyte, this behavior could be explained by the higher PS-solubility of the electrolyte, which leads to a higher PS-shuttle. However, this explanation is not applicable for the LiFSI-electrolyte. Therefore, the lower viscosity during cycling (due to the lower PS-solubility) could be the reason for the lower coulombic efficiency of the LiFSI-electrolyte, which facilitates the PS-shuttle. This is underlined by the fact that the viscosity of the PS-saturated LiFSI-solution is four times lower than for the other electrolyte solutions.

Post-mortem Analyses were performed for the cells after 50 cycles, as shown in Figure S3. For the imide-based salts and LiTf, quite similar greyish lithium anode surfaces are observed. LiFSI leads, in accordance with the Li vs Li tests, to the most uniform surface, whereas a more irregular distribution of lithium can be observed for LiTFSI, LiBETI and LiTf. The

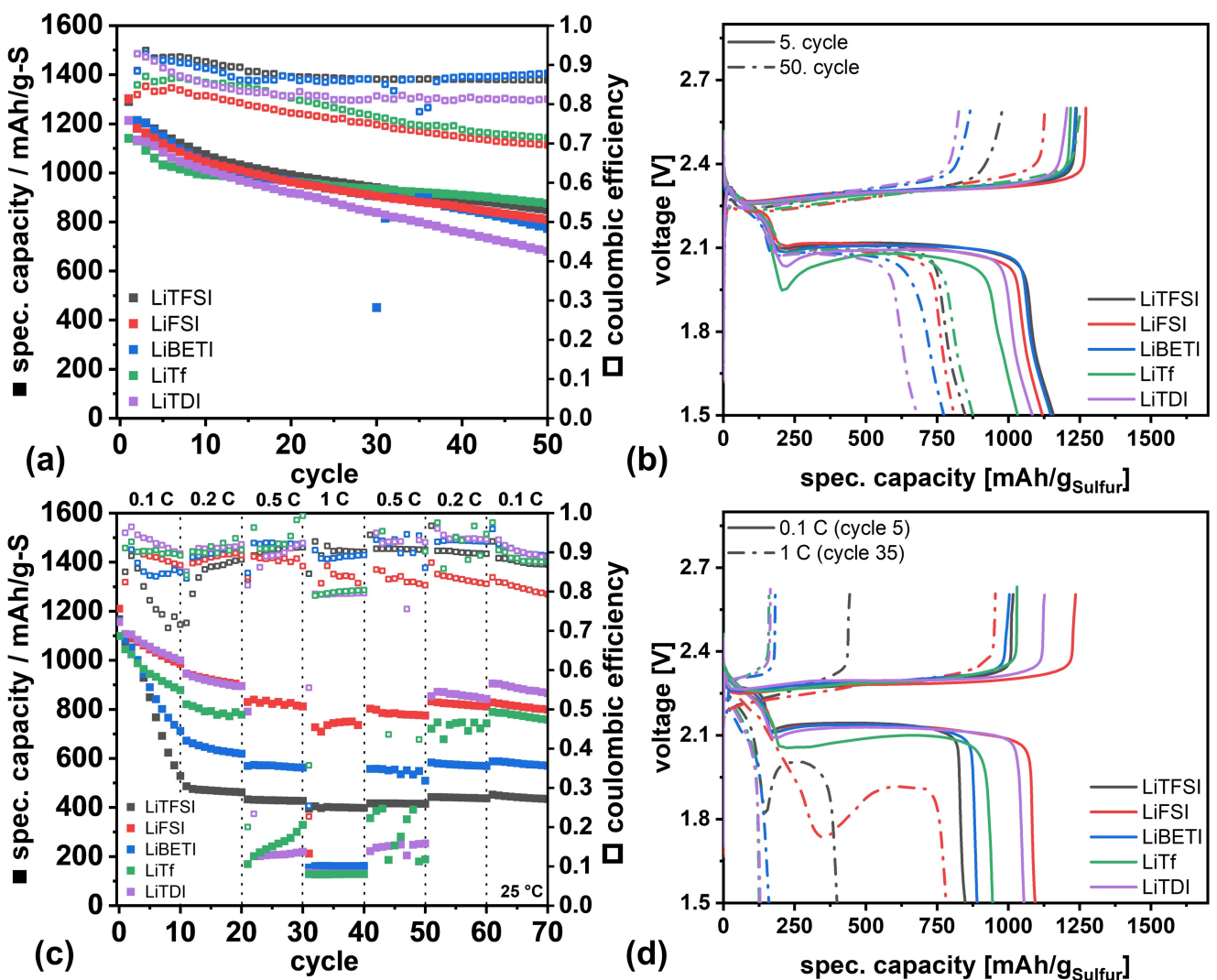


**Figure 4.** Galvanostatic cycling of the different lithium salts in coin cells at 25 °C using DME/TTE 1/1 with 1 M lithium salt as electrolyte. a) + b) cycling at 0.1 C using a C/S cathode with a sulfur loading of 2.2 mg/cm<sup>2</sup>. c) + d) rate capability tests using a C/S cathodes with a sulfur loading of 1.0 mg/cm<sup>2</sup>.

strongest decomposed lithium surface is formed in the LiTDI-cells, which is also in good agreement with the Li vs Li tests. The dark coloration of the anode indicates stronger electrolyte degradation. Therefore, LiTDI might not be the lithium salt of choice for lithium metal anodes. In addition, SEM-measurements were carried out to further characterize the surface of the lithium metal anodes. The anodes were washed before the measurements (Figure S3, Supporting Information) in order to remove electrolyte residues (especially lithium salt). However, the washing step lead also to a wash out of some SEI-components as can be seen by the images in Figure S3, despite the use of a solvent with low solvating ability (hexyl methyl ether). The SEM-images, shown in Figure S4 show again that LiFSI leads to the most compact lithium growth in comparison to the further imide-based salts LiTFSI and LiBETI. For LiTf and LiTDI, a higher content of the SEI might be washed out as can be already seen by the comparison of the photos. However, there are still a higher amount of cracks on the surface of the LiTDI cell.

Further coin cell testing at 0.1 C was also performed in a longer cycling range of 120 cycles, shown in Figure S5. The results confirm that the use of LiTf leads to the highest capacity retention despite the very low coulombic efficiency of less than 70% in the last 80 cycles. LiTFSI and LiBETI lead to the second highest capacity retention after 120 cycles, which agrees well with the similar structure of both lithium salts. LiTDI and LiFSI show the lowest capacity retention, whereas the degradation of the lithium metal anode might be an explanation for the LiTDI-electrolyte. In case of LiFSI, the even further decreasing coulombic efficiency might lead to an increased loss of sulfur/polysulfides on the lithium anode surface. Since this electrolyte shows a rather small PS-solubility, the readdressing of this sulfur species might be more difficult as in case of LiTf. However, it must be noted that these results were obtained in coin cells using high excess of lithium and also excess amount of electrolyte (E:S = 7 µl/mg-S). Thus, performance under lean conditions might differ.

In contrast to the cycling at constant C-rate, the lithium salts influence the rate capability of the cells strongly, shown in Figure 4(c) and (d). Additional voltage profiles can be found in Figure S2. Different C-rates from 0.1 C to 1 C (0.1 C, 0.2 C, 0.5 C, 1 C) were considered during discharge, while the charging rate was kept constant at 0.1 C. Unfortunately the higher loaded cathode of the test performed before shows only a limited rate capability. Therefore, a different electrode with a sulfur loading of 1 mg-S/cm<sup>2</sup> was used for the rate capability studies. Boenke *et al.*<sup>[13,49]</sup> could show that using these cathodes enables multilayered pouch cells with a high rate capability and specific energy.

Due to the lower sulfur loading, the coin cell tests had to be carried out at a higher electrolyte to sulfur ratio (E:S=11 µl/mg-S), in order to fill the high dead volume of coin cells. Here, a strong correlation between the rate performance and the ionic conductivities of the electrolytes can be observed. Accordingly, the LiFSI-electrolyte shows the highest rate capability resulting in a high sulfur utilization up to 1 C. The high C-rate of 1 C leads to a higher overpotential in comparison to 0.1 C, especially at the second plateau. Unfortunately, the two other imide-based salts LiBETI and LiTFSI show an unexpected fast degradation already in the first 10 cycles at 0.1 C. This behavior is reproducible and remains so far unexplained. It might be caused by a different precipitation mechanism of sulfur species by these salts in combination with the different cathode composition since such a behavior was not observed in the first test at 0.1 C. However, despite this fast degradation, LiTFSI is the only salt besides LiFSI, which leads to the formation of a short second plateau at 1 C. In addition, LiTFSI and LiBETI show also at 0.5 C a higher sulfur utilization than LiTDI and LiTf. For LiTf, an overpotential can be already observed at 0.2 C resulting in a lower sulfur utilization in comparison to LiFSI and LiTDI. Therefore, the sulfur utilization at higher C-rates correlates well with the ionic conductivity of the five electrolyte solutions in the order LiFSI>LiTFSI≈LiBETI>LiTDI>LiTf. Regarding the voltage profiles, a voltage dip is observed between the two plateaus at 1 C for the LiTFSI- and the LiFSI-electrolyte, this can be related to the increasing concentration of polysulfides in the electrolyte during the first plateau, which results in slower ion transport. In addition, also the starting nucleation of Li<sub>2</sub>S could lead to an increase in overpotential. In case of the LiFSI electrolyte, the influence of polysulfides should be minimal based on the initially performed electrolyte characterizations. Thus, the occurrence of the voltage dip could indicate that polysulfide formation during cycling might be different or that indeed Li<sub>2</sub>S nucleation leads to high overpotentials at higher C-rates. However, operando-measurements are needed to clarify the reaction mechanism of these electrolytes. Post-mortem analysis was performed also for these coin cells, shown in Figure S6.

The observations correspond with the ones observed before for the testing at 0.1 C since LiFSI shows again the less decomposed surface. In general, stronger degradation is observed, which can be explained by the higher currents applied during the rate capability test. As already mentioned, the coin cell tests were carried out under electrolyte excess

conditions, which is beneficial for the kinetics since dissolution of polysulfides in the electrolyte, would lead only to minor changes of the electrolyte properties. This could be shown before by Boenke *et al.* in the same cell setup using SOTA-DME/DOL-electrolyte and a SPSE (HME/DME).<sup>[13]</sup> Thus, in order to validate the obtained results also under practical conditions, multilayer LiS-pouch cells (5 double-sided cathodes) were built using lean electrolyte conditions (E:S=3 µl/mg-S) as well as a thin lithium metal anode (50 µm). The results are shown in Figure 5. Since the rate capability of the lithium salts LiTf, LiTDI was already quite low under flooded conditions and LiBETI showed a lower rate capability than LiTFSI in combination with a lower ionic conductivity the focus was set on a comparison between LiTFSI and LiFSI. Interestingly, in pouch cells, the LiTFSI-electrolyte still shows a linear degradation at 0.1 C. However, the effect is drastically lowered in comparison to the coin cell results, reaching still quite high sulfur utilization of 1000 mAh/g after the 10 cycles at 0.1 C. Therefore, the capacity loss might be related to the cell setup especially the constant pressure on the pouch cell stack – whereas in the coin cell, only a spacer was employed. By increasing the current, cycling at 0.2 C and 0.5 C is also possible with only a low decrease of sulfur utilization. This comes along with a marginal overpotential at 0.2 C, which further increases slightly at 0.5 C with the second plateau still at 2.0 V. At 1 C, only very low sulfur utilization is observed since the second plateau is not formed and the voltage limit of 1.5 V is reached during the voltage dip. By lowering the C-rate again in the following cycles, a regeneration of the sulfur utilization is observed with values of 800 mAh/g to 900 mAh/g.

The pouch cells containing the LiFSI-electrolyte in comparison with the LiTFSI-cells show a lower degradation at 0.1 C. Consequently, the sulfur utilization is also higher at the following increasing C-rates. The strong difference between both electrolytes is the performance at 1 C, whereas LiTFSI-electrolyte is not capable to reach high sulfur utilization (only 200 mAh/g), the LiFSI-cells lead to a high sulfur utilization of 850 mAh/g. In addition to this phenomenal result, the overpotential of the cell is still quite low with the second plateau at 1.95 V, which is very important in order to reach high energy densities. Such a performance, to the best of our knowledge, has so far never been shown in literature under lean electrolyte conditions, underlining the importance of this study. Regarding the coulombic efficiency, again moderate values are detected for both electrolyte compositions, in accordance to the coin cell results, with values around 90%. For the LiFSI-electrolyte a strong decrease of the coulombic efficiency after 50 cycles is observed, which might indicate a stronger electrolyte decomposition in comparison to LiTFSI. Post mortem analysis was also conducted for the multilayer pouch cells, shown in Figure 6. A picture of a representative lithium metal anode and a separator was taken. The lithium anode surface of the LiTFSI-cell appears darker than observed for the LiFSI-cell, indicating a stronger decomposition of the electrolyte, which supports the observations made in coin cells. To conclude the results, LiFSI seems to be the salt of choice in terms of cells with high power requirements. This is

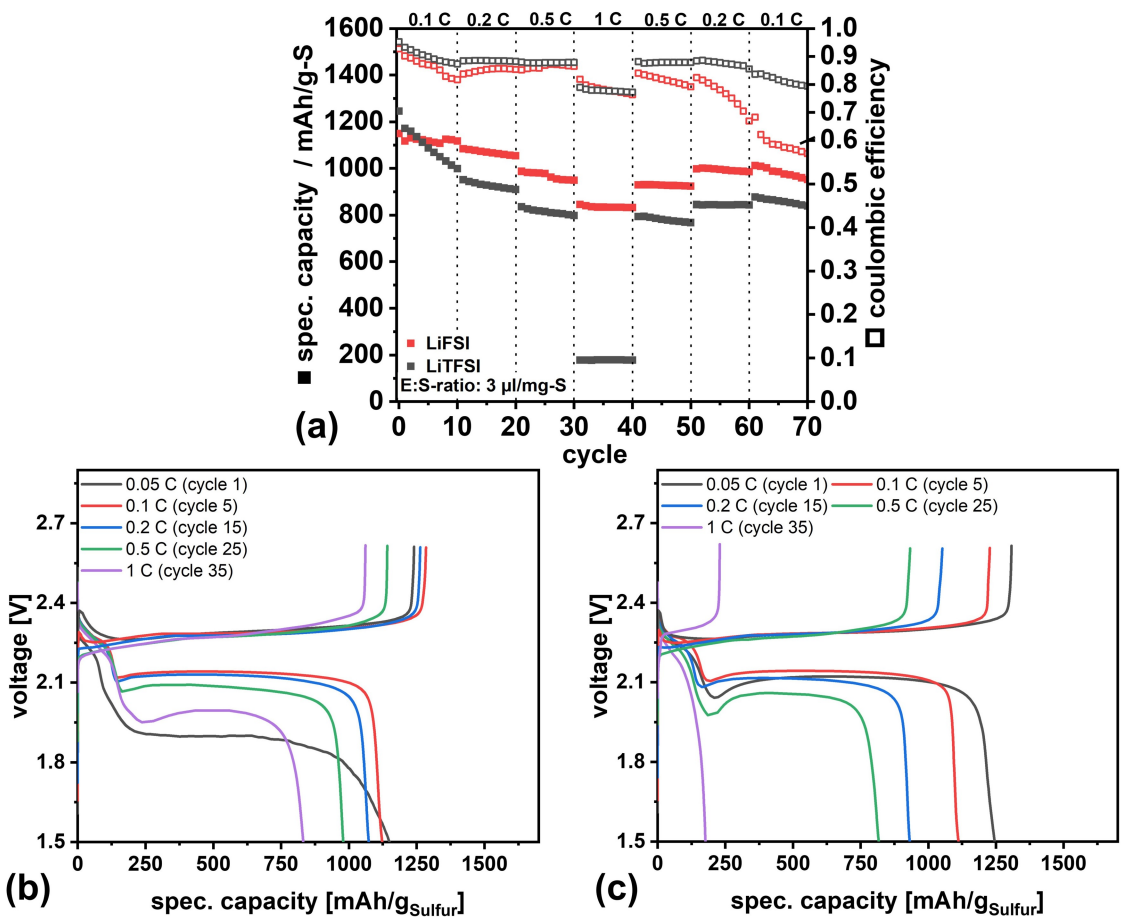


**Figure 5.** (a) Galvanostatic cycling of multi-layered pouch cells under lean-electrolyte conditions ( $E:S = 3 \mu\text{l}/\text{mg-S}$ ) with varying C-rates during discharge (0.1 C–1 C) of LiTFSI- and LiFSI-electrolyte, using a C/S-cathode with a sulfur loading of  $1.0 \text{ mg-S/cm}^2$ , (b) voltage profiles of LiFSI-cell, (c) voltage profiles of LiTFSI-cell.

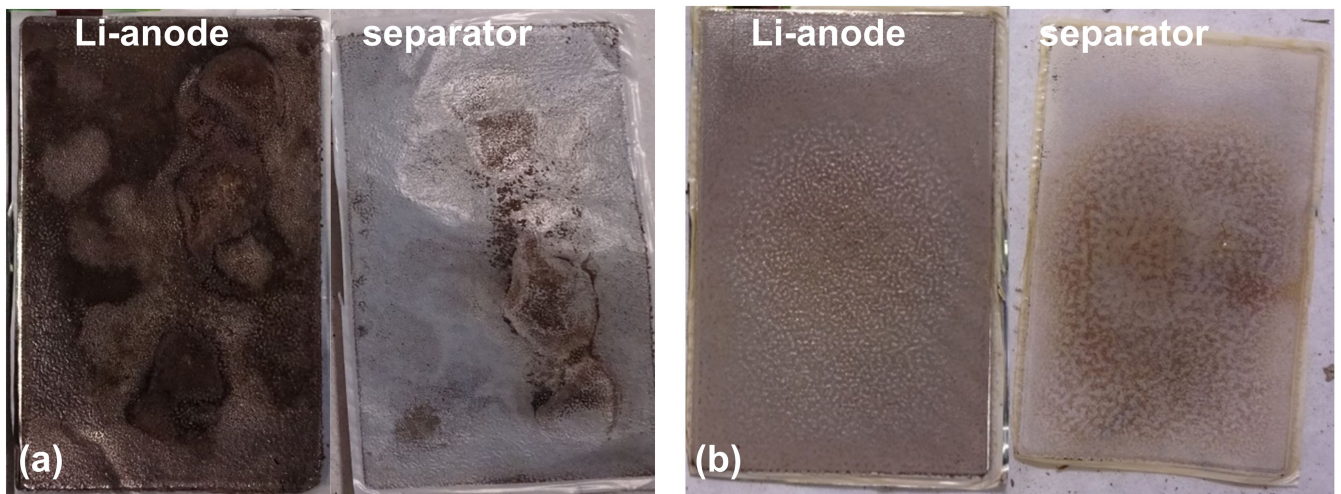


**Figure 6.** Post mortem analysis of the cycled lithium anodes and separators: (a) LiTFSI-cell, (b) LiFSI-cell.

related to the high ionic conductivity of the electrolyte as well as the low influence of polysulfides on the electrolyte properties. In future studies, an adaption of the solvent

system would be beneficial in order to decrease the electrolyte density as well as potential costs (use of TTE).

## Conclusions

In this study, we focused on the influence of the lithium salt in an adapted solvent mixture on the performance of Li–S-batteries. The investigation of electrolyte properties show that mainly the ionic conductivity is strongly affected by the lithium salt whereas density and viscosity are dominated by the solvents of the electrolyte and the total salt concentration. Interestingly, we could show that also the polysulfide solubility is affected by the lithium salt. In comparison to reference LiTFSI (and LiBETI as structure analogs), especially LiTf shows higher PS-solubility. LiFSI, in contrast, shows nearly no polysulfide solubility. Therefore, also the electrolyte properties in electrolytes saturated with polysulfides are only marginally affected in case of LiFSI, making it a very promising choice for lean electrolyte conditions. Interestingly, by evaluating the electrolytes in coin cells at 0.1 C, only minor differences in the capacity retention could be observed. In contrast, by performing rate capability tests with increasing C-rates, the lithium salts did show a strong influence on the performance. As a result, the ionic conductivity of the electrolyte could be related to the rate capability of the cells in the order LiFSI > LiTFSI ≈ LiBETI > LiTDI > LiTf. The results of the coin cell testing were subsequently transferred into multilayered pouch cells, and the high rate capability of LiFSI was confirmed, even under very lean electrolyte conditions (3 µl/mg-S). These findings might be a promising step in order to increase the rate capability of Li–S-batteries for real world applications. The adaption of the solvent composition, especially in terms of the hydrofluoroether TTE, is a promising step in order to decrease the electrolyte density and maximize the specific energy.

## Experimental Section

### Materials

DME (Gotion) was dried using molecular sieve, TTE was used as received. Before the electrolyte preparation, Karl-Fischer titration was carried out to ensure that the water content is below 20 ppm. The lithium salts used, LiTFSI (Gotion), LiFSI (Arkema), LiBETI (Iolitec), LiTf (Sigma Aldrich), LiTDI (Arkema), were dried prior use at 120 °C in a vacuum oven over night. The electrolytes were prepared in an Ar-filled glovebox ( $O_2 < 0.1$  ppm,  $H_2O < 0.1$  ppm). The concentration of the electrolytes refers to 1 mol salt per liter solvent (system).

### Electrolyte Characterization

Ionic conductivity of the electrolytes was determined with a four-pole graphite measuring LF400 electrode (GHM Messtechnik GmbH) in a sealed glass cell filled with 4 ml of electrolyte. The temperature was controlled by a silicon oil bath.

A Haake Rheostress 1 rheometer from Thermo Fisher Scientific Inc. was used to determine the viscosity of the electrolytes at 25 °C using a double cone geometry with an angle of 1°.

The density of the electrolytes was measured with a small graduated flask (1 ml).

The influence of polysulfides was studied by preparing polysulfide-saturated solutions. Therefore, Li<sub>2</sub>S and sulfur were added in stoichiometric ratio to the electrolyte to form Li<sub>2</sub>S<sub>6</sub> in excess. The oversaturated solutions were filtered through a syringe filter and properties were determined as performed for the pure electrolytes. In addition, the polysulfide solubility was determined gravimetrically by oxidizing polysulfides chemically under basic conditions with H<sub>2</sub>O<sub>2</sub> to sulfate-anions. These could then be precipitated with Ba(NO<sub>3</sub>)<sub>2</sub> under acidic conditions as BaSO<sub>4</sub>. The precipitate was washed three times and dried at 120 °C.

### Electrochemical Characterization

The C/S-cathodes used for the galvanostatic cycling at 0.1 C were produced as described earlier.<sup>[16,24]</sup> The sulfur loading is 2.2 mg-S/cm<sup>2</sup> and the sulfur content is 60%. The C/S-cathodes with a sulfur loading of 1.0 mg/cm<sup>2</sup> electrodes were obtained via a melt infiltration process as described by Boenke *et al.*<sup>[49]</sup> The cathodes were composed of a CNT-buckypaper with a CNT-loading of 1.0 mg/cm<sup>2</sup> and a sulfur loading of 1.0 mg-S/cm<sup>2</sup>, corresponding to a sulfur-content of 50%.

Symmetrical Li vs. Li tests were carried out in coin cells using 250 µm lithium chips (d = 16.5 mm), a 12 µm PE separator and 30 µl of electrolyte. A current density of 0.5 mA/cm<sup>2</sup> was applied for 2 h to obtain a total capacity of 1 mAh/cm<sup>2</sup>.

Galvanostatic cycling at 0.1 C (1 C = 1672 mAh/g) was performed with the C/S-cathode (2.2 mg-S/cm<sup>2</sup>) in coin cells using a 12 µm PE separator and the same lithium chips as mentioned earlier. The electrolyte amount was adjusted to an E:S-ratio of 7 µl/mg-S. After an initial cycle (0.05 C discharge, 0.1 C charge), the cells were cycled symmetrical with 0.1 C in a voltage range of 1.5 V to 2.6 V.

Rate capability tests were performed using the C/S-cathode with the lower sulfur-loading of 1 mg-/cm<sup>2</sup> in the same coin cell setup. An electrolyte amount of 20 µl had to be used (corresponds to an E:S ratio of 11 µl/mg-S) in order to completely fill the dead volume of the cell.

The coin cells were cycled asymmetrical with varying C-rate during discharge (0.1 C, 0.2 C, 0.5 C and 1 C and back to 0.1 C) with 10 cycles per C-rate and 0.1 C as constant charging rate. Again, the voltage range was 1.5 V to 2.6 V.

Pouch cell testing was performed using 5 double layered C/S-cathodes (1 mg-S/cm<sup>2</sup>, 32.7 cm<sup>2</sup> per side), 12 µm PE separator and 50 µm lithium (per cathode side). An E:S-ratio of 3 µl/mg-S was applied. Evaluation was performed for the LiTFSI and the LiFSI-electrolyte.

All cell tests were carried out at 25 °C. For pouch cell evaluation, a constant uniaxial pressure of 0.31 MPa was applied.

SEM images of the cycled lithium metal anodes were taken using a scanning electron microscope JSM-6610LV (JEOL GmbH).

### Supporting Information

Supporting Information is available from the Wiley Online Library or from the author.

## Acknowledgements

The authors wish to thank Peter Fleischer for pouch cell assembly as well as *post mortem*-analysis. Furthermore, many thanks go to Lisa Pillar for electrolyte preparations and characterization and to Anke Krawietz for cathode preparation. This work has received funding from the Federal Ministry of Education and Research, Germany (BMBF), in the project SkaLiS (03XP0398). Open Access funding enabled and organized by Projekt DEAL.

## Conflict of Interests

The authors declare no conflict of interest.

## Data Availability Statement

The data that support the findings of this study are available from the corresponding author upon reasonable request.

**Keywords:** lithium-sulfur · electrolyte · pouch cell · lithium salt · hydrofluoroether

- [1] T. Li, X. Bai, U. Gulzar, Y.-J. Bai, C. Capiglia, W. Deng, X. Zhou, Z. Liu, Z. Feng, R. Proietti Zaccaria, *Adv. Funct. Mater.* **2019**, *29*, 1901730.
- [2] H. Kim, G. Jeong, Y.-U. Kim, J.-H. Kim, C.-M. Park, H.-J. Sohn, *Chem. Soc. Rev.* **2013**, *42*, 9011.
- [3] a) OXIS Energy, "OXIS Energy is close to achieving 500 Wh/kg and is targeting 600 Wh/kg with Solid State Lithium Sulfur technology", **2020**; b) F. Schmidt, M. Fiedler, T. Arlt, A. De, F. Hoffmann, F. Wilde, S. Dörfler, B. Schumm, T. Abendroth, H. Althues, et al., *Energy Technol.* **2023**, *11*, 2300518; c) Q. Cheng, Z.-X. Chen, X.-Y. Li, L.-P. Hou, C.-X. Bi, X.-Q. Zhang, J.-Q. Huang, B.-Q. Li, *J. Energy Chem.* **2023**, *76*, 181.
- [4] S. Dörfler, S. Walus, J. Locke, A. Fotouhi, D. J. Auger, N. Shateri, T. Abendroth, P. Härtel, H. Althues, S. Kaskel, *Energy Technol.* **2021**, *9*, 2000694.
- [5] a) K. Zhu, C. Wang, Z. Chi, F. Ke, Y. Yang, A. Wang, W. Wang, L. Miao, *Front. Energy Res.* **2019**, *7*, 12436; b) T. Cleaver, P. Kovacic, M. Marinescu, T. Zhang, G. J. Offer, *J. Electrochem. Soc.* **2018**, *165*, A6029.
- [6] M. Zhao, B.-Q. Li, H.-J. Peng, H. Yuan, J.-Y. Wei, J.-Q. Huang, *Angew. Chem. Int. Ed.* **2020**, *59*, 12636.
- [7] Y. Liu, Y. Elias, J. Meng, D. Aurbach, R. Zou, D. Xia, Q. Pang, *Joule* **2021**, *5*, 2323.
- [8] a) G. Bieker, V. Küpers, M. Kolek, M. Winter, *Commun Mater.* **2021**, *2*, 436; b) J. Han, Y. Li, S. Li, P. Long, C. Cao, Y. Cao, W. Wang, Y. Feng, W. Feng, *Sustain. Energy Fuels* **2018**, *2*, 2187; c) T. Tonoya, H. Ando, N. Takeichi, H. Senoh, T. Kojima, H. Hinago, Y. Matsui, M. Ishikawa, *J. Phys. Chem. C* **2023**, *127*, 10038.
- [9] W.-J. Chen, B.-Q. Li, C.-X. Zhao, M. Zhao, T.-Q. Yuan, R.-C. Sun, J.-Q. Huang, Q. Zhang, *Angew. Chem. Int. Ed.* **2020**, *59*, 10732.
- [10] J. Zhou, Y. Guo, C. Liang, L. Cao, H. Pan, J. Yang, J. Wang, *Chem. Commun. (Camb.)* **2018**, *54*, 5478.
- [11] a) G. Ma, Z. Wen, M. Wu, C. Shen, Q. Wang, J. Jin, X. Wu, *Chem. Commun. (Camb.)* **2014**, *50*, 14209; b) J. Castillo, J. A. Coca-Clemente, J. Rikarte, A. Sáenz de Buruaga, A. Santiago, C. Li, *APL Mater.* **2023**, *11*, 010901; c) H.-K. Jing, L.-L. Kong, S. Liu, G.-R. Li, X.-P. Gao, *J. Mater. Chem. A* **2015**, *3*, 12213; d) C. Sun, X. Huang, J. Jin, Y. Lu, Q. Wang, J. Yang, Z. Wen, *Power Sources* **2018**, *377*, 36.
- [12] a) N. Deng, W. Kang, Y. Liu, J. Ju, D. Wu, L. Li, B. S. Hassan, B. Cheng, *J. Power Sources* **2016**, *331*, 132; b) B.-W. Zhang, B. Sun, P. Fu, F. Liu, C. Zhu, B.-M. Xu, Y. Pan, C. Chen, *Membranes* **2022**, *12*, 790; c) X. Zhou, Q. Liao, J. Tang, T. Bai, F. Chen, J. Yang, *J. Electroanal. Chem.* **2016**, *768*, 55; d) J. Liu, J. Wang, L. Zhu, X. Chen, Q. Ma, L. Wang, X. Wang, W. Yan, *Chem. Eng. J. (Amsterdam, Neth.)* **2021**, *411*, 128540; e) H.-J. Peng, D.-W. Wang, J.-Q. Huang, X.-B. Cheng, Z. Yuan, F. Wei, Q. Zhang, *Adv. Sci. (Weinheim, Ger.)* **2016**, *3*, 1500268.
- [13] T. Boenke, S. Kirchhoff, F. S. Reuter, F. Schmidt, C. Weller, S. Dörfler, K. Schwedtmann, P. Härtel, T. Abendroth, H. Althues, et al., *Nano Res.* **2023**, *16*, 8313.
- [14] J. Scheers, S. Fantini, P. Johansson, *J. Power Sources* **2014**, *255*, 204.
- [15] D. Aurbach, E. Pollak, R. Elazari, G. Salitra, C. S. Kelley, J. Affinito, *J. Electrochem. Soc.* **2009**, *156*, A694.
- [16] C. Weller, S. Thieme, P. Härtel, H. Althues, S. Kaskel, *J. Electrochem. Soc.* **2017**, *164*, A3766.
- [17] C. Qu, Y. Chen, X. Yang, H. Zhang, X. Li, H. Zhang, *Nano Energy* **2017**, *39*, 262.
- [18] a) L. Cheng, L. A. Curtiss, K. R. Zavadil, A. A. Gewirth, Y. Shao, K. G. Gallagher, *ACS Energy Lett.* **2016**, *1*, 503; b) H. Ye, Y. Li, *Nano Res. Energy* **2022**, *1*, e9120012.
- [19] C. Weller, J. Pampel, S. Dörfler, H. Althues, S. Kaskel, *Energy Technol.* **2019**, *20*, 9821.
- [20] a) K. Sun, Q. Wu, X. Tong, H. Gan, *ACS Appl. Energ. Mater.* **2018**, *1*, 2608; b) L.-P. Hou, X.-Q. Zhang, N. Yao, X. Chen, B.-Q. Li, P. Shi, C.-B. Jin, J.-Q. Huang, Q. Zhang, *Chem* **2022**, *8*, 1083; c) W.-J. Chen, C.-X. Zhao, B.-Q. Li, Q. Jin, X.-Q. Zhang, T.-Q. Yuan, X. Zhang, Z. Jin, S. Kaskel, Q. Zhang, *Energy Environ. Mater.* **2020**, *3*, 160; d) C.-C. Su, M. He, R. Amine, Z. Chen, K. Amine, *Angew. Chem. Int. Ed.* **2018**, *57*, 12033.
- [21] M. Cuisinier, P.-E. Cabelguen, B. D. Adams, A. Garsuch, M. Balasubramanian, L. F. Nazar, *Energy Environ. Sci.* **2014**, *7*, 2697.
- [22] a) N. Azimi, W. Weng, C. Takoudis, Z. Zhang, *Electrochem. Commun.* **2013**, *37*, 96; b) C.-C. Su, M. He, R. Amine, K. Amine, *Angew. Chem. Int. Ed.* **2019**, *58*, 10591.
- [23] L. Suo, Y.-S. Hu, H. Li, M. Armand, L. Chen, *Nat. Commun.* **2013**, *4*, 1481.
- [24] S. Dörfler, H. Althues, P. Härtel, T. Abendroth, B. Schumm, S. Kaskel, *Joule* **2020**, *4*, 539.
- [25] a) X. Kong, Y. Kong, X. Liao, S. Liu, Y. Zhao, *Sustain. Energy Fuels* **2022**, *6*, 3658; b) T. Liu, H. Li, J. Yue, J. Feng, M. Mao, X. Zhu, Y.-S. Hu, H. Li, X. Huang, L. Chen, et al., *Angew. Chem. Int. Ed.* **2021**, *60*, 17547; c) Q. Cheng, W. Xu, S. Qin, S. Das, T. Jin, A. Li, A. C. Li, B. Qie, P. Yao, H. Zhai, et al., *Angew. Chem. Int. Ed.* **2019**, *58*, 5557; d) H. S. Yang, D.-M. Kim, Y. Kim, Y. J. Lee, K. T. Lee, *ChemElectroChem* **2021**, *8*, 2321; e) T. Liu, Z. Shi, H. Li, W. Xue, S. Liu, J. Yue, M. Mao, Y.-S. Hu, H. Li, X. Huang, et al., *Adv. Mater.* **2021**, *33*, e2102034.
- [26] R. Younesi, G. M. Veith, P. Johansson, K. Edström, T. Vegge, *Energy Environ. Sci.* **2015**, *8*, 1905.
- [27] G. Liu, Q. Sun, Q. Li, J. Zhang, J. Ming, *Energy Fuels* **2021**, *35*, 10405.
- [28] a) S. Nanda, A. Manthiram, *Adv. Energy Mater.* **2021**, *7*, 2003293; b) K. Sun, N. Li, D. Su, H. Gan, *J. Electrochem. Soc.* **2019**, *166*, A50.
- [29] K. S. Han, J. Chen, R. Cao, N. N. Rajput, V. Murugesan, L. Shi, H. Pan, J.-G. Zhang, J. Liu, K. A. Persson, et al., *Chem. Mater.* **2017**, *29*, 9023.
- [30] H. Kim, F. Wu, J. T. Lee, N. Nitta, H.-T. Lin, M. Oschatz, W. I. Cho, S. Kaskel, O. Borodin, G. Yushin, *Adv. Energy Mater.* **2015**, *5*, 1401792.
- [31] a) Z. Jiang, Z. Zeng, W. Hu, Z. Han, S. Cheng, J. Xie, *Energy Storage Mater.* **2021**, *36*, 333; b) W. Shin, L. Zhu, H. Jiang, W. F. Stickle, C. Fang, C. Liu, J. Lu, X. Ji, *Mater. Today* **2020**, *40*, 63; c) J. Zheng, X. Fan, G. Ji, H. Wang, S. Hou, K. C. DeMella, S. R. Raghavan, J. Wang, K. Xu, C. Wang, *Nano Energy* **2018**, *50*, 431; d) J. Zheng, G. Ji, X. Fan, J. Chen, Q. Li, H. Wang, Y. Yang, K. C. DeMella, S. R. Raghavan, C. Wang, *Adv. Energy Mater.* **2019**, *9*, 1803774; e) Y. Zheng, F. A. Soto, V. Ponce, J. M. Seminario, X. Cao, J.-G. Zhang, P. B. Balbuena, *J. Mater. Chem. A* **2019**, *7*, 25047; f) L. Yoshida, Y. Matsui, M. Deguchi, T. Hakari, M. Watanabe, M. Ishikawa, *ACS Appl. Mater. Interfaces* **2023**, *15*, 37467.
- [32] X. Ren, L. Zou, X. Cao, M. H. Engelhard, W. Liu, S. D. Burton, H. Lee, C. Niu, B. E. Matthews, Z. Zhu, et al., *Joule* **2019**, *3*, 1662.
- [33] K. Xu, C. A. Angell, *J. Electrochem. Soc.* **2002**, *149*, A920.
- [34] D. Di Lecce, V. Marangon, H.-G. Jung, Y. Tominaga, S. Greenbaum, J. Hassoun, *Green Chem.* **2022**, *24*, 1021.
- [35] A. Gupta, A. Bhargav, A. Manthiram, *Adv. Energy Mater.* **2019**, *9*, 1803096.
- [36] Q. Pang, A. Shyamsunder, B. Narayanan, C. Y. Kwok, L. A. Curtiss, L. F. Nazar, *Nat. Energy* **2018**, *3*, 783.
- [37] Z. Yue, H. Dunya, S. Aryal, C. U. Segre, B. Mandal, *J. Power Sources* **2018**, *401*, 271.
- [38] F. Schmidt, A. Korzenko, P. Härtel, F. S. Reuter, S. Ehrling, S. Dörfler, T. Abendroth, H. Althues, S. Kaskel, *J. Phys. Energy* **2022**, *4*, 14004.
- [39] H. Pan, X. Wei, W. A. Henderson, Y. Shao, J. Chen, P. Bhattacharya, J. Xiao, J. Liu, *Adv. Energy Mater.* **2015**, *5*.

- [40] J. Chen, K. S. Han, W. A. Henderson, K. C. Lau, M. Vijayakumar, T. Dzwinel, H. Pan, L. A. Curtiss, J. Xiao, K. T. Mueller, et al., *Adv. Energy Mater.* **2016**, *6*, 1600160.
- [41] a) M. Baek, H. Shin, K. Char, J. W. Choi, *Adv. Mater.* **2020**, *32*, e2005022; b) H. Chu, J. Jung, H. Noh, S. Yuk, J. Lee, J.-H. Lee, J. Baek, Y. Roh, H. Kwon, D. Choi, et al., *Adv. Energy Mater.* **2020**, *10*, 2000493; c) B. Yang, H. Jiang, Y. Zhou, Z. Liang, T. Zhao, Y.-C. Lu, *ACS Appl. Mater. Interfaces* **2019**, *11*, 25940.
- [42] J. W. Dibden, J. W. Smith, N. Zhou, N. Garcia-Araez, J. R. Owen, *Chem. Commun. (Camb.)* **2016**, *52*, 12885.
- [43] F. S. Reuter, C.-J. Huang, Y.-C. Hsieh, S. Dörfler, G. Brunklaus, H. Althues, M. Winter, S. D. Lin, B.-J. Hwang, S. Kaskel, *Batteries & Supercaps* **2021**, *4*, 347.
- [44] a) A. Nakanishi, K. Ueno, D. Watanabe, Y. Ugata, Y. Matsumae, J. Liu, M. L. Thomas, K. Dokko, M. Watanabe, *J. Phys. Chem. C* **2019**, *123*, 14229; b) R. Glaser, O. Borodin, B. Johnson, S. Jhulki, G. Yushin, *J. Electrochem. Soc.* **2021**, *168*, 90543.
- [45] H.-B. Han, S.-S. Zhou, D.-J. Zhang, S.-W. Feng, L.-F. Li, K. Liu, W.-F. Feng, J. Nie, H. Li, X.-J. Huang, *J. Power Sources* **2011**, *196*, 3623.
- [46] a) J. Qian, W. A. Henderson, W. Xu, P. Bhattacharya, M. Engelhard, O. Borodin, J.-G. Zhang, *Nat. Commun.* **2015**, *6*, 6362; b) Y. Leng, S. Ge, R. S. Longchamps, X.-G. Yang, T. Liu, C.-Y. Wang, *J. Electrochem. Soc.* **2020**, *167*, 110543; c) R. Miao, J. Yang, X. Feng, H. Jia, J. Wang, Y. Nuli, *J. Power Sources* **2014**, *271*, 291; d) R. Miao, J. Yang, Z. Xu, J. Wang, Y. Nuli, L. Sun, *Sci. Rep.* **2016**, *6*, 21771; e) M. Wang, L. Huai, G. Hu, S. Yang, F. Ren, S. Wang, Z. Zhang, Z. Chen, Z. Peng, C. Shen, et al., *J. Phys. Chem. C* **2018**, *122*, 9825.
- [47] H. Chu, H. Noh, Y.-J. Kim, S. Yuk, J.-H. Lee, J. Lee, H. Kwack, Y. Kim, D.-K. Yang, H.-T. Kim, *Nat. Commun.* **2019**, *10*, 188.
- [48] a) M. W. Wagner, C. Liebenow, J. O. Besenhard, *J. Power Sources* **1997**, *68*, 328; b) C. Yan, X.-B. Cheng, C.-Z. Zhao, J.-Q. Huang, S.-T. Yang, Q. Zhang, *J. Power Sources* **2016**, *327*, 212.
- [49] T. Boenke, P. Härtel, S. Dörfler, T. Abendroth, F. Schwotzer, H. Althues, S. Kaskel, *Batteries & Supercaps* **2021**, *4*, 989.

Manuscript received: March 5, 2024

Revised manuscript received: June 15, 2024

Accepted manuscript online: June 20, 2024

Version of record online: August 2, 2024